

Adventures with a bistatic chirp and CW radar

Andrew Martin¹ VK3OE/VK3OER

Introduction

Since the development of the chirp radar for amateur use was first reported on the VKLogger [1] in January 2010 together with the publication of the concept in DUBUS [2], many experiments and measurements using the SpectrumLab [3] software have been conducted to understand the capability of this radar. Some of these results were reported at the most recent GippsTech conference [4]. During this process some basic operating techniques have been developed to easily verify each measurement to be certain about what is being measured. Some surprising results have also emerged that show how capable is the chirp radar technique. These results could also serve as a basis for the revision of some Es theories, especially theories relating to long distance propagation on 50 MHz.

It has also been found that the combination of chirp and CW modes is very useful to ascertain the nature of the reflecting object. If the signal is returned from a stationary object, then of course it has no Doppler shift. But if the object is moving, the return signal will have a Doppler shift which, in chirp mode, will cause a range error. Objects such as aircraft have a very specific Doppler shift, while moving ionospheric irregularities can have a very wide range of Doppler shifts from one target. In these cases, the use of the chirp and CW modes is most helpful to ascertain the actual distance to the moving object.

During 2011, I developed a separate internet connected remote station (VK3OER), which is at a distance of 145 km from VK3OE. This station is very useful for receiving radar signals sent from VK3OE (in Bistatic Radar mode) and allows the received audio signals to be processed easily in real time.

The radar has been used on all the amateur bands from 14 MHz to 144 MHz to find out what can be achieved and what are the limitations. Most of the measurements have concentrated on the bands of 28 MHz and 50 MHz. 2 m has proved to be the most difficult band because there were only limited ducting opportunities available to test this band during the 2011-2012 summer ducting season.

The HPSDR group is developing the Hermes SDR transceiver with chirp mode built in, together with GPS timing and frequency control, which will enable direct and accurate measurement of distance to any chirp source or reflector. This development will significantly enhance the functionality of amateur chirp radars and

greatly assist in the more widespread application of the chirp radar capability [5, 6].

Doppler Shift Errors and System Values

Doppler shift is of great concern when using the chirp radar as any Doppler shifted returns will be subject to a range error during processing. These range errors occur because any frequency shift of the return signal makes the return signal appear in a different place than where it actually is. This range error can be readily calculated. The Doppler shift, Fd , is given by:

$$Fd = 2vFt/c \quad \text{Hz (1)}$$

where v is the velocity of the object (for radar, a receding object will produce a negative Doppler shift with respect to the transmitted signal), Ft is the transmit frequency and c is the speed of light. The Doppler shift is measured in CW mode.

The range error, Re , in seconds, when in chirp mode is then given by

$$Re = -Fd/(dF/dt) \quad \text{s (2)}$$

where dF/dt is the chirp rate in Hz per second.

The actual location of the object, Ra , with the measured Doppler shift is then given by

$$Ra = Rm - Re \quad \text{s (3)}$$

where Rm is the measured range (will be negative with respect to the direct signal if the Doppler shift is positive for a positive chirp rate dF/dt).

As the output from the chirp radar mode is in seconds, the distance can be easily calculated by multiplying the time by 150,000 to get km in the backscatter mode and by 300,000 to get distance in the forward scatter mode.

Doppler shifted returns can look like static reflections in chirp mode and may be misinterpreted as they can appear in odd places, such as earlier than the direct signal. To resolve this, it is necessary to turn the radar to CW mode so that any Doppler shifted return signals can be identified and the Doppler shift measured. The actual range to the object can then be calculated from the above equations, allowing return signals to be correctly located and identified.

The system gain, G_s , can be calculated from:

$$G_s = TXp + TXant + RXant - RXsen \quad \text{dB (4)}$$

where TXp is the transmit power, $TXant$ is the transmit antenna gain in dBi (cable losses included), $RXant$

is the receiver antenna gain in dBi and RX_{sen} is the noise power of the receiver in a 2 kHz bandwidth when connected to an antenna. TX_p and RX_{sen} are normally expressed in dBm.

The complex receiver chirp processing gain, G_p , is given by:

$$G_p = 10 * \log(BT) + 3 + 10 * \log(Nchirp) \quad \text{dB (5)}$$

where B is the chirp bandwidth, T is the length of the chirp and $Nchirp$ is the number of chirps averaged.

The chirp radar system gain, G_c , is then given by:

$$G_c = G_s + G_p \quad \text{dB (6)}$$

The path loss, Pl , in radar mode can be estimated from:

$$Pl = G_c - S / Nc \quad \text{dB (7)}$$

where S/Nc is the signal to noise ratio of the received chirp.

The estimated S/N for a one way contact is:

$$S / N = G_s - Pe \quad \text{dB (8)}$$

where Pe is the estimated one way path loss given by:

$$Pe = 20 * \log(d) + 20 * \log(f) - 147.55 + Es_l + Rd \quad \text{dB (9)}$$

where d is the distance in metres, f is the frequency in Hz, Es_l is the Es layer reflection loss and Rd is the D layer absorption loss, which applies for each D layer transit in daylight. The Es reflection loss for each reflection is assumed to be around 2 dB on 28 MHz and 50 MHz, while the D layer absorption loss is assumed to be around 1.5 dB at 28 MHz and 3 dB on 50 MHz for each D layer transit. The earth surface reflection loss is assumed to be close to 0 dB.

For all the 50 MHz radar measurements, $TX_{ant} = 12$ dBi Yagi @ 25 m with $TX_p = 50$ watts. The receive antenna is 145 km away, and $RX_{ant} = 12$ dBi Yagi @ 8 m. Assuming an RX_{sen} level of -129 dBm in a 2 kHz bandwidth (noise limited, not the receiver sensitivity), this gives a system gain G_s of 200 dB on 50 MHz. In chirp mode, a chirp from 500 Hz to 2500 Hz over one second is used, which, when averaged for ten seconds, gives a G_p of 46 dB. This is added to G_s to give a G_c of 246 dB on 50 MHz.

For the 28 MHz measurements, $TX_{ant} = 8$ dBi Yagi @ 24 m with $TX_p = 50$ watts. The receive antenna is 145 km away, and $RX_{ant} = 4$ dBi Yagi @ 6 m. Assuming a RX_{sen} level of -121 dBm in a 2 kHz bandwidth, this gives a G_s of 180 dB. In chirp radar mode, $G_p = 46$ dB is added to give a $G_c = 226$ dB on 28 MHz.



www.ttssystems.com.au

Phone: 03 5977 4808 Email: info@ttssystems.com.au

Your Australian reseller for:



YouKits

New Products coming soon

AVAILABLE NOW

Hard Drawn Copper Wire, Insulators, Dipole Centres
Open Wire Transmission Line, Spreaders, Kevlar Guy Line
Spiderbeam Fibreglass Poles, Baluns and Switches



Meanwell power supplies
Diamond products
Daiwa products
Technical books
Amidon products
Custom cables made to order

Compliments of the Season from TTS

In backscatter mode, the backscatter coefficient, G_b , required from the backscatter object to obtain the measured S/N_c , is given by:

$$G_b = P_l - 2 * P_e \quad \text{dB (10)}$$

The backscatter coefficient was measured on 14 MHz using the chirp bistatic radar and found to be close to 43 dB at a distance of 1300 km. This value compares favourably with the maximum value of around 40 dB measured on 16 MHz at a distance of 1500 km by Steele [22]. This result gives considerable confidence that the measuring techniques used here are reasonable.

The backscatter coefficient, G_b , of an area can be estimated from

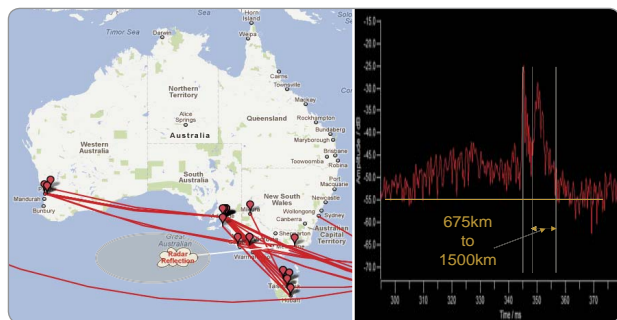
$$G_b = 20 * \log_{10}(4 * \pi * A_b * C_c / \lambda^2) \quad \text{dB (11)}$$

where A_b is the backscatter area and C_c is the correlation coefficient for the backscatter.

A very convenient program for generating chirp and CW signals is SpectrumLab [3]. It also has a built-in chirp receiver. In the case where better analysis of the received signals is required, the received audio chirp can be recorded by SpectrumLab and then analysed in Matlab®.

Es Backscatter Measurements on 50 MHz

Backscatter measurements of Es using chirp and CW modes have been made on 28 MHz and 50 MHz. The 28 MHz measurements are relatively easier to make than measurements at 50 MHz because the probability of Es propagation at 28 MHz is higher than at 50 MHz. Further, it is often the case when using the radar at 50 MHz that no returns are received, even though there is 50 MHz propagation as evidenced by contacts. This is because of layer rippling and focusing [7], which is more evident at 50 MHz than at 28 MHz. The layer rippling and focusing often causes the remote receiver site to be in an Es "hole", especially when the radar transmitter is 145 km away. Figure 1: 26 November 2011, open to WA on 50 MHz, VK



Logger [8] showing spots and the location of the radar backscatter return, the radar reflection. Also shown is the chirp radar received data from the direction of 260 degrees using SpectrumLab. The noise level is about -55 dB.

Shown in Figure 1 is a radar result from the direction of 260 degrees on 50 MHz. The radar was first tried in the direct path to Perth at 275 degrees but no backscatter return was received. The antennas were

then turned further south and the maximum backscatter return was in the direction of 260 degrees. The direct signal is at 345 ms in Figure 1, with a chirp signal to noise ratio (S/N_c) of 30 dB, which is treated as zero distance, while the backscatter return is between 4.5 ms and 10 ms later than the direct signal, with an S/N_c of about 27 dB. This gives a backscatter footprint of between 675 km and 1500 km in the direction of 260 degrees, as shown in Figure 1, and indicates that the backscatter signal is most probably from an Es layer and not from the F layer. By using equations 4 to 10 above, the sea surface gain required for this level of backscatter at 800 km can be calculated to be around 42 dB. The VKLogger radar spot [8] is also shown for the same time.

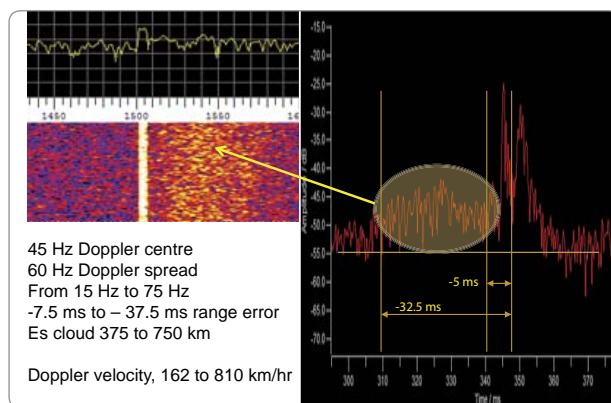


Figure 2: Measuring the Doppler shifted component of the return signal using SpectrumLab. The Doppler is centred at about +45 Hz from the direct signal with a spread of 60 Hz, from 15 Hz to 75 Hz. The direct signal with no Doppler shift is the bright line at 1505 Hz.

Also shown in Figure 1 is a spread out signal at up to 12 dB S/N_c , which appears before the direct signal. This is a Doppler shifted signal that is easily measured by changing the radar to CW mode. The result is shown in Figure 2. The direct signal with no Doppler shift is at 1505 Hz.

Using equation 1 gives the velocity of the backscatter object of between 162 km/hr and 810 km/hr. This velocity is close to typical wind speeds in the E layer and indicates that there is a large amount of turbulence and shear that is resulting in a backscatter signal from the Es layer. This backscatter is the mode often used for communication on 50 MHz and the Doppler shift causes the often reported distortion.

Equation 2 provides a range error value when the radar is used in chirp mode. This range error of between -37.5 ms and -7.5 ms can now be used in conjunction with equation 3 and the measured range of -32.5 ms and -5 ms to give actual ranges of 5 ms to 2.5 ms. This equates to the backscatter object being between 750 km and 225 km away. If these distances are doubled, we get distances of between 1500 km and 450 km, very close to the distances of the ground return footprint reported earlier. It is interesting to note that the highest Doppler frequency comes from the most distant part of the Es irregularity.

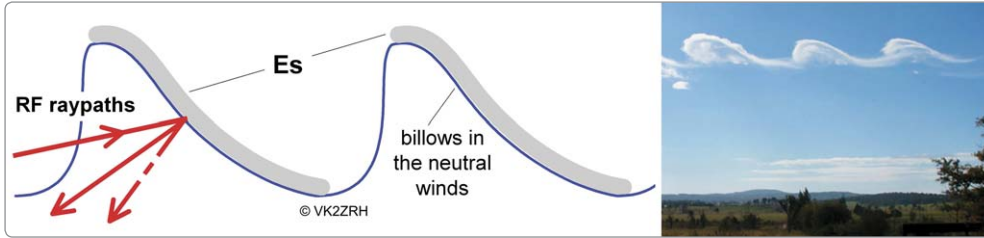


Figure 2a: From [9]. Illustration of Kelvin-Helmholtz billows in Es at around 100 km altitude as an agent of back and side-scatter. The picture on the right is a visual indication of Kelvin-Helmholtz billows in the lower atmosphere, probably around 3 to 5 km altitude. This is the mechanism that produces the billows, crinkles, ripples or wrinkles in Es (as various authors have described).

The backscatter S/N_c from Figure 2 is about 12 dB at -18 ms from the direct signal. This part of the backscatter is about 500 km away. Using the above equations, we can calculate that the backscatter coefficient is around 17 dB to get the measured S/N_c . If it is assumed that the backscatter coefficient is around 0.01^2 for Es, then the backscatter object is about 10,000 m² in area (100 m x 100 m, equation 11) and seems reasonable, given a vertical wavelength of the Es ripples of about 2 km [21]. This is a rather different result for Es backscatter than for backscatter from the surface of the Earth, see later.

It is thus assumed that the Doppler backscatter is directly from the Es ripples; the mechanism is shown in Figure 2a [9, 10]. The picture (added by Harrison) is from Wikipedia Commons [10].

A further interesting issue is that the Es is south of the direct path to Perth for the contacts shown in Figure 1. This could indicate that the contacts were not made by the direct great circle path but by side-scatter from the Es by layer rippling [9] caused by the windshear at the height of the Es layer. This is further supported by the fact that the ground backscatter return is from a path further south than the direct path to Perth. The contacts to Perth shown in Figure 1 are probably via two hops via side-scatter from the irregularities in the Es layer.

This example has thus shown that backscatter with Doppler shift from Es is possible and that side-scatter from the Es ripples is also possible.

In Figure 3, recordings of using the radar in CW mode to measure the velocity of the Es ripples are

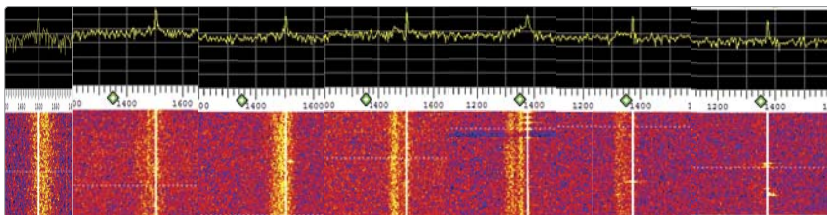


Figure 3: 26 November 2011, 260 degrees, 30 minutes of backscatter signals with 7 records showing Doppler shift measurement in 50 MHz CW radar mode. Records are 1 to 7 from the left. Recorded from 45 minutes after data of Figure 2. Direct signals with zero Doppler shift are the bright lines.

shown for a 30 minute period. The first record on the left shows a positive Doppler shift that evolves through zero to show a strong negative Doppler shift by record 4. At record 5, this has split into two, which is probably due to vortex-like structures induced by wind shear [11]. By record 6, the

Doppler shifted signal is getting weaker, and by record 7 it has gone. This is explained as follows, from [11] "The Doppler width of the spectra is associated with the scatterers' velocity distribution inside the ionospheric volume illuminated by the radar beam. When turbulence is the main cause of backscatter, the spectral width gives an idea of the intensity of the turbulence." This is shown in Figure 4.

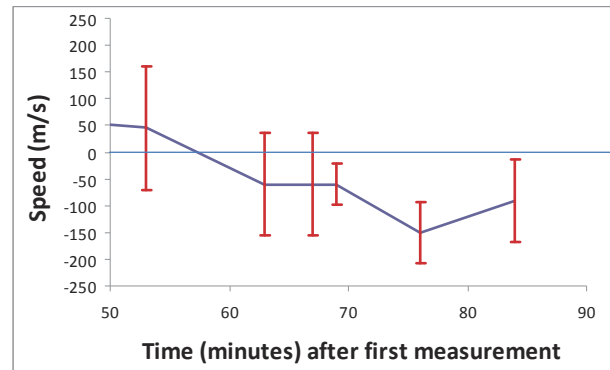


Figure 4: Doppler velocity evolution and spread from the backscatter 50 MHz CW measurements. Time is in minutes after first measurement of Figure 3 was taken.

In Figure 4, the maximum line of sight velocity is -150 m/s and is considerably higher than the velocities of 20 m/s reported in [11]. This probably because the measurement reported in [11] is from a vertically sounding (53 MHz) radar while the data of Figure 4 is from a horizontal measurement, probably indicating that the principal wind flow in the E layer is in the horizontal direction, producing higher line of sight Doppler shift. Speeds of up to 150 m/s were reported in [12].

The line of sight wind starts off towards the CW radar and then evolves to recede before disappearing. The measured speeds are probably the result of the crinkles moving in sheets of Es. Whitehead [13] states that "we may picture it as a fairly smooth horizontal sheet of ionization just a few kilometres thick, extending

over 1000 km in horizontal size but with these slight ripples in it". When the signals are focused in particular directions with moving ripples, the result looks like moving clouds. This is discussed in [14, 20]. Kennedy and Zimmerman [14] state that "As the free electrons are dragged across the magnetic field, at roughly a 90° angle to the field, this produces a sideways electromagnetic force that bends the electron paths either upward or downward into orbits circling the field lines rather than continuing to move along with the wind."

Further, the width of the Doppler in Figure 4, of up to 70 m/s, is in the range of 20 to 150 m/s reported in [12]. As the width of the Doppler spread is related to turbulence, it is reasonable that the Doppler spread will be similar for a horizontal or vertical measurement.

Further results similar to those above were obtained on 18 and 21 January 2012, which served to confirm that the measurement results described above could be repeated.

Es backscatter measurements on 28 MHz

The chirp radar measurement in Figure 5 shows Es backscatter returns obtained at an azimuth of 60 degrees out to a distance of 11,100 km. There are seven (7) distinct returns evident, indicating seven (7) hops. At the time of the measurement, there was a blanketing Es event on the Canberra and Sydney ionosondes, so no returns from the F layer are evident. The first two F layer hops' nulls would appear at around 3100 km and 6200 km. At both these locations, there is a clear return, which indicates that at these points, Es is involved. Further, all the hop distances are consistent with typical Es hop distances and are shown in Table 1. Because the average distances are shown in Table 1, it cannot be assumed that these are the distances of each hop. Indeed, it is most likely that multiple modes are occurring in hops 1 and 2 so that any assumptions about individual distances may be incorrect. It is also obvious that the peak amplitude return for each hop is not at an exact multiple of any particular distance.

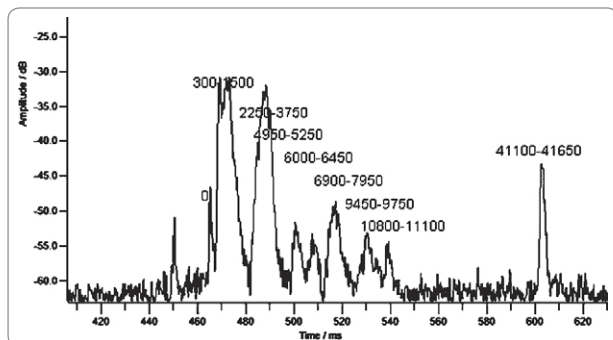


Figure 5: 28 MHz chirp backscatter measurement made @ 05:38UTC on 13 June 2012. The direction is 60 degrees. Distances are marked in km for each return, Zero distance is the direct signal. The signal at 450 ms arriving before the direct signal is a Doppler shifted return from an aircraft.

If it is assumed that all hops have an equal distance of around 1500 km (10 ms) it is difficult to get a reasonable fit to match the distances shown for each return. There are also distinct nulls between each hop, reinforcing the fact that each radar return is a separate entity and that multiple backscatter signals are not overlapping, which would otherwise fill-in between each hop.

The signal returns out to 550 ms are all backscatter returns, so the distance is found by multiplying the time in ms from the direct signal by 150. The signal at 603 ms is a forward scatter result for once around the Earth, so the distance is obtained by multiplying the time in ms from the direct signal by 300. The signal at 603 ms in Figure 5 is from once around the earth and is probably achieved by mixed Es and F layer propagation with a dominant F layer guided mode; see the discussion later in this article.

Another interesting observation from Figure 5 is that between hops 1 and 2, the loss is very low. Further, there is a reduction in level between hops 2 and 3 of about 20 dB (10 dB in each direction), but after that there is only minimal loss between each hop for hops 3 to 7. The number of reflections for the 7th hop is a total of 14 Es reflections (out and back) and a total of 12 surface reflections. The return from each hop is by surface backscatter. The backscatter occurs only once for each return signal. The large number of out and back reflections illustrates that it may be possible to have 14 hops in a row, to over 20,000 km, it just needs the Es to be present as a sufficiently large horizontal sheet of ionization.

There will also be some signal attenuation in the D layer for each transit. At each reflection point, the loss is very low because of the almost grazing reflection angles [7, 15]. In order to make up the propagation loss from the radar over a distance of 22,000 km (which is twice the loss for 11,000 km) there needs to be some gain in the propagation path.

Hop	Distance of hop km	Time of day	Signal to Noise S/Nc
1	900	Day	35 dB
2	2100	Day	33 dB
3	2100	Evening	12 dB
4	1125	Night	10 dB
5	1227	Night	17 dB
6	2148	Night	10 dB
7	1350	Night	8 dB

Table 1: Hop distances for each of the 7 hops, together with S/Nc estimated from Figure 5. As the returns for the first two hops are spread, the hop distances are taken from the middle of each return for the first two hops and may not represent the actual path reflection point used to obtain the longer distance returns.

This probably occurs when the 10m signal is backscattered from the sea surface at a low angle such as would be the case for Es originated signals. The backscatter surface needs to have scatters in the order of half a wavelength (5m in this case) to be effective.

Hop	Calculated Path Loss	Measured Path Loss <i>PI</i>	Backscatter coefficient required <i>G_b</i>
1	244 dB	191 dB	53 dB
2	268 dB	193 dB	75 dB
3	297 dB	214 dB	83 dB
4	305 dB	216 dB	89 dB
5	311 dB	209 dB	102 dB
6	318 dB	216 dB	102 dB
7	323 dB	218 dB	105 dB

*Table 2: The calculated radar path losses assume free space path loss. Loss is also added to each hop to account for D layer transits and reflection losses plus a step loss of 10dB between hops 2 and 3 to account for the step loss in between those hops Figure 5. Each hop loss in then doubled to get the total radar loss. The measured loss is calculated by using the received S/Nc in Table 1 together with the system parameters outlined earlier. The extra backscatter coefficient, *G_b*, required to get the measured S/Nc is shown in the last column.*

The backscatter surface gain, equation 11, can be applied to estimate the size of the surface needed to achieve the backscatter coefficients required in Table 2. If the backscatter correlation coefficient, *C_c* is 0.001 (see footnote 1, earlier), an area around 10,000 square km (100 km x 100 km) is sufficient to provide the required gains. As the sea surface is involved for every backscatter point, these values seem reasonable. The sea surface roughness will also affect the backscatter level. There is an increase in the backscatter coefficient with increasing distance which is probably related to the spread of the footprint at increasing distance.

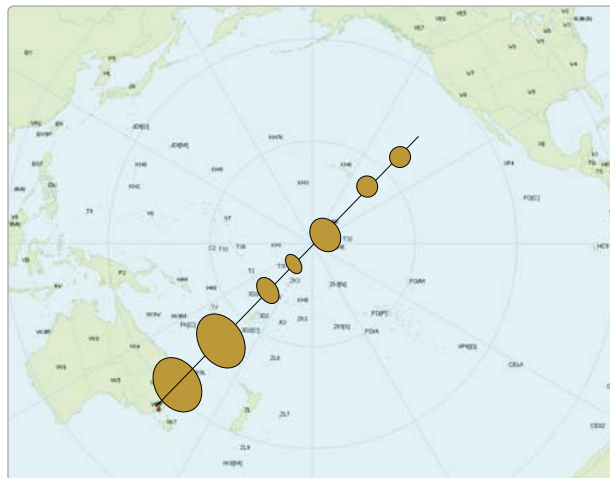
At the time of the measurements shown in Figure 5, there were Es contacts on 50 MHz between VK3 and VK4 at levels up to S9. The one way path loss to the 1st hop is estimated to be 122 dB on 28 MHz (half the calculated path loss for the first hop in Table 2). If the system gain of 180 dB is used for a 2 kHz bandwidth, then the one way signal level on 28 MHz will be approximately S9 (S/N = 180 dB - 122 dB = 58 dB), which is similar to the 50 MHz one way signal level at the time.

The S/Nc from Table 1 to the 7th hop at 11,000 km is 8 dB, giving a measured radar path loss of 218 dB (equation 7). An estimated one way path loss of 161.5 dB (half the calculated path loss for the seventh hop in Table 2), provides the calculated overall radar path loss of 323 dB, requiring a backscatter coefficient (*G_b*) of 323 dB - 218 dB = 105 dB. Thus, the estimated S/N for a one way 28 MHz contact (neglecting the backscatter coefficient as it is not used for a one way contact) is *G_s* - 161.5 dB = 18.5 dB or close to S3 (assuming that the one way path loss estimate of 161.5 dB is correct).

The three longest hop distances shown in Table 2 are all over 2100 km. The fact that the hops are not all of equal length is attributed to the tilting and focusing that occurs due to wind shear and changes in the Es layer height over the 11,000 km path [7, 13].

From a conventional concept, for Es to support multi-hop propagation over 11,000 km suggests that seven Es “clouds” needed to be in exactly the right position at the right time. This is most unlikely and a better explanation may be that there was a wrinkled sheet of Es over the whole area (“crinkles, ripples or wrinkles” in the electron/ion sheet, as Prof. David Whitehead once put it [13]). As discussed earlier, the individual Es reflection points will then be controlled by the Es sheet height at each point, the nature of the “wrinkles” and the path geometry. As shown earlier in the section about Es 50 MHz, it is possible that Es side scatter is possible along the path so the results shown in Figure 5 may not be as a result of direct (great circle) path propagation.

Figure 6: Location and approximate size of each of the Es hops in the direction of 60 degrees. The first four hops



are before the equator crossing while there are three hops beyond the equator. The skip distances are typical of Es propagation and no F layer propagation is involved.

The result of Figure 5 also shows that there is multi-hop long distance nEs propagation during the Southern winter solstice. It is thus likely that the same mechanism is present around the summer solstice when many contacts have been made between VK and North/South America in recent years. Many of these contacts were made when the sunspot numbers were very low.

Figure 6 shows the approximate locations of Es hop together with the approximate size of each backscatter return. The seven hops measured clearly have a path that crosses the Equator. This has not previously been thought to be possible as it had been assumed that the F layer was required for the Equatorial transit. This is clearly not the case as the hop distances are typical of those seen for Es propagation.

Further, Figure 7 shows multi-hop Es on 50 MHz, possibly out to a distance of more than 10,000 km. The bistatic chirp radar provides further evidence that nEs is indeed one of the long distance modes, this time also crossing the equator on 50 MHz. The S/Nc at 10,000 km is 15 dB, giving a measured radar path loss of 231 dB (equation 7). An estimated one way path loss of 154.5 dB provides an overall radar path loss of 309 dB, requiring a backscatter coefficient (G_b) of 309 dB – 231 dB = 77 dB. Thus, the estimated S/N for a one way 50 MHz contact (neglecting the backscatter coefficient) is $G_s - 154.5 \text{ dB} = 45.5 \text{ dB}$ or close to S7 (assuming that the one way path loss estimate is correct). By the same process, a one way contact on 50 MHz at 1100 km made at the same time as the measurement of Figure 7 would give S/N of around 64 dB or S9+15 dB. In Figure 7, the filling-in between the principal returns indicates that multiple propagation modes are present so that, after about 5000 km, the radar returns are completely smeared out. This is in contrast to the returns of Figure 5 where the individual returns are very distinct.

It is thus likely that nEs is an often-used mode for long distance 50 MHz contacts and that the short-path summer solstice propagation (SSSP) hypothesis put forward by Higasa [16] has some limitations.

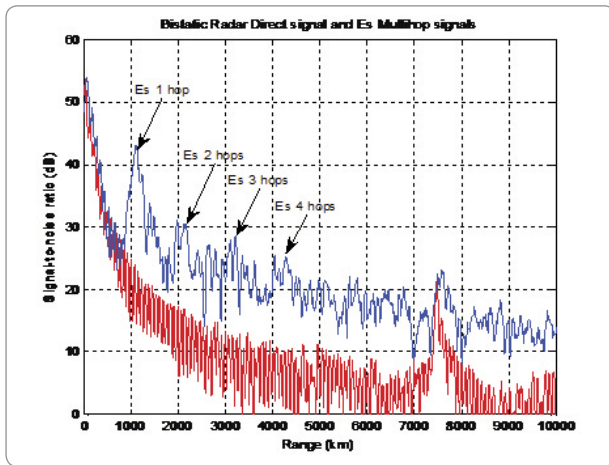


Figure 7: 0230 UTC on 22 January 2010 from a direction of 50 degrees. nEs measurement from [2] showing clear evidence of 4 Es hops. When the return signal is compared to the response with no signal (red) there is clear evidence of returns out to a distance of 10,000 km. The return at 7,600 km is an equipment spurious. After 1000 km there is a substantial amount of in-fill between each hop, indicating the presence of multiple propagation modes.

The nEs/SSSP is also discussed extensively by Harrison in [7] and he indicates that “To me, Higasa’s hypothesis fails on too many key points. We know that the paths are not completed by F2 propagation or by tropospheric refraction/ducting. The remaining option is that SSSP propagation is supported by multi-hop Es (nEs, Figure 25). The next step is to find the evidence to match the

contacts.” The nEs measurements shown in Figure 5 (28 MHz) and 7 (50 MHz) may indeed be the evidence that supports the nEs hypothesis put forward by Harrison in [7] and sought by Kennedy and Zimmerman [14]. If the 50 MHz long distance contacts reported were indeed by nEs, as this evidence suggests, then the concerns about distortion, excessive attenuation and scattering being limiting factors [14, 16] can be dismissed.

Comparing 28 MHz and 50 MHz Es measurements

The question that arises from the 28 MHz measurements is: can the 28 MHz backscatter measurements be used for an indicator for 50 MHz propagation? To try to answer this, closely-spaced chirp radar measurements (one minute apart) were made on 28 and 50 MHz, the results of which are shown in Figure 8.

The return signals are very closely aligned, indicating that very similar results for Es reflections and surface backscatter can be obtained on 28 MHz and 50 MHz. This is very encouraging. The concept is that the 28 MHz chirp radar can be used as an indicator for 50 MHz propagation.

The 28 MHz signal in Figure 8 (top) appears at a slightly shorter distance than the 50 MHz signal (bottom) by about 150 km), indicating that the skip distance on 28 MHz is shorter than the skip distance on 50 MHz. The same effect could also be present in the result of Figure 5, resulting in a slightly longer range for 50 MHz than was measured at 28 MHz.

By using the point for maximum S/Nc of 1500 km for 28 MHz and 50 MHz, the required sea surface

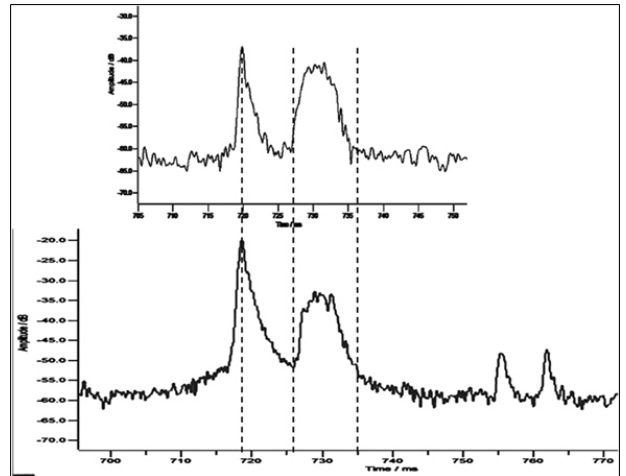


Figure 8: Closely spaced (1 minute) measurements using the chirp radar on 28 MHz, top, and 50 MHz, bottom, at 04:15 on 3rd July 2012. The two traces have been arranged so that the direct signals for each are in the same place and the time scales are the same. The first return in both pictures is Earth surface backscatter via an Es cloud at around 100 km altitude. The ground backscatter return is from between 1050 km with an angle of arrival of about 9 deg, and from 2450 km, with an angle of arrival close to 0 deg [9].

backscatter coefficient is estimated to be 56 dB for 28 MHz and 57 dB for 28 MHz. This represents an area of about 1 km wide and 75 km long (75 km is the minimum resolvable range), using the correlation coefficient of 0.001 as before. Contacts on 50 MHz at the time over the same path were producing S9 reports. A calculation using the measured results suggests S/N in 2 kHz of 62 dB, S9+10 dB.

The S/N on 50 MHz is around 27 dB, while the S/N on 28 MHz is around 22 dB. The two returns on 50 MHz at 765 and 762 ms are from aircraft, and appear to be at a great distance because of range errors due to Doppler shift.

Around The World in 137.83 ms on 28 MHz

Figure 9 shows a 28 MHz chirp radar measurement out to a distance of 100,000 km. Three returns are evident, at 7000 km, 41,350 km (137.83 ms) and 82,700 km (275.66 ms = 2 x 137.83 ms). Matlab® was used to obtain these values from the leading edge of the pulses. The first 'spike' is a first-hop surface backscatter via the F layer, while the second spike is a first *around-the-world* (ATW), and the third spike a second ATW. Such ATW signals were first measured by Hess in 1948 [17] where he reported a propagation time of 137.78 ms. Frequencies of between 10 and 20 MHz were used. The guided mode of F layer propagation is well described by Carera et al in 1970 [18]. The time measurements of first and second ATW signals shown in Figure 9 represent an error of 0.05 ms when compared to those of Hess, even

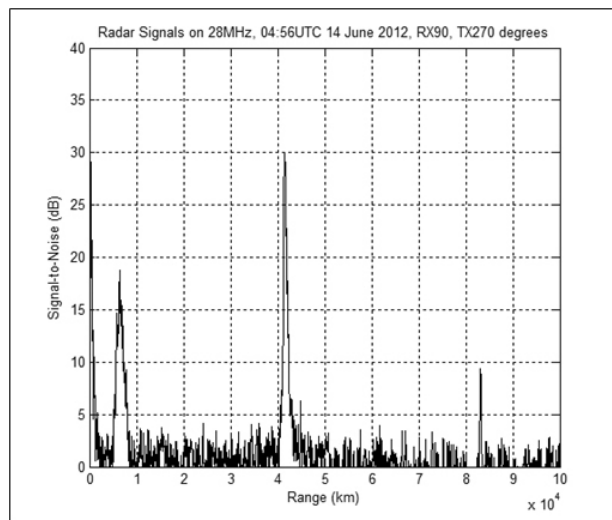


Figure 9: 28 MHz chirp radar measurements at 04:56 UTC on 14 June 2012. Transmitting at 270 degrees, receiving at 90 degrees. Signal processing gain is 46 dB, which would represent S/N of -16 dB in a 2 kHz bandwidth. X axis distance scale is 300 km/ms. The first around-the-world return has its leading edge at 41,350 km (137.83 ms) and the second around-the-world return has its leading edge at 82,700 km (275.66 ms). The signal at 7000 km is in fact a first hop Earth surface backscatter signal via the F layer at a distance of 3500 km.

though the measurement of Figure 9 is at 28 MHz. This indicates that the ATW propagation mechanisms on 10 to 20 MHz are the same as those on 28 MHz. Further, there is no Doppler shift on the ATW signal as there are no other significant signals anywhere near the ATW signal position that would indicate a range error induced Doppler shift.

The first and second ATW signals are about 300 km wide (at the -3 dB points following the leading edge of the signal), which indicates that there are some delayed components up to 1ms following along from the first signal (dispersion). By comparison, the direct signal at 0 km is only 75 km wide (at the -3dB points), which is at the limit of the resolution for a 2 kHz-wide chirp. The fact that the first and second ATW signals have the same amount of dispersion indicates that once established, the ATW signals are not further dispersed by additional modes such as additional F-layer-to-surface hops. The direct result of this is that, once established in the F layer, the signals are guided by the F layer throughout the path.

The ATW signals travel from 1275 km to 1575 km further than the surface of the Earth, which represents an increase in the radius that the radio waves travel, ranging from 203 km to 250 km, at the height of the F layer. This is a further confirmation that the signals stay at or very close to the F layer indicating a guided mode of propagation and not a multi-hop mode as that would cause an increase in distance greater than that measured.

The azimuth angles used for the transmit and receive antennas are close to those reported by Fenwick and Villard [21]. The prediction of long path ATW signals by HamCap [19] also confirms that the azimuth angles used are close to correct. An ATW contact could have been made on 28 MHz CW as the S/N of -16 dB (30 - 46 dB) in a 2 kHz bandwidth is close to the minimum level useable for CW, for a 200 Hz bandwidth the S/N of the CW signal would be -6 dB: contact completed.

The result also indicates that ATW signals may also be present on 50 MHz and a measurement campaign is now in place to see if this can be achieved. If there is 40 dB extra loss on 50 MHz than on 28 MHz, then with 2 x 12 dBi antennas and 100 watts, the chirp radar S/N should be around 5 dB, which is detectable. The next step would then be to make a 50 MHz CW contact using this mode to make the longest possible long path contact of 40075 km. Time will tell.

Aurora backscatter measurements on 28 MHz

On the 29th of June 2012 I was looking for around the world signals when some extra returns were seen. The antennas were peaked on the signal at 220 degrees. There were three extra signals clearly evident in Figure 10, sea surface backscatter via Es at a distance of 1500 km, an auroral backscatter signal at a distance of 3900 km and a Doppler range shifted auroral signal a further 26 ms away.

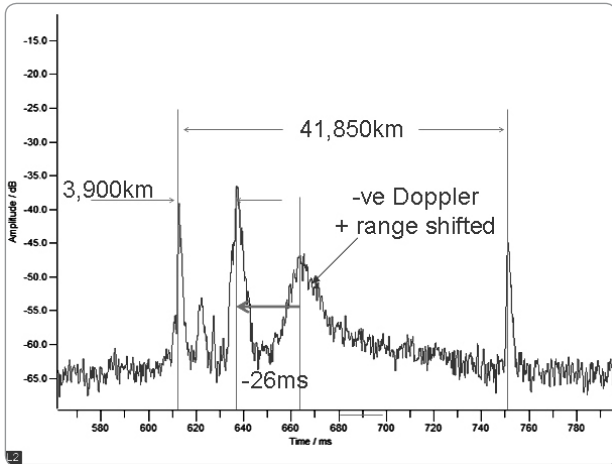


Figure 10: 28 MHz chirp backscatter radar measurements at 220 degrees, 04:40UTC, 29 June 2012. The direct signal is at 612ms. The signal at 622ms is backscatter from the sea surface via Es at a distance of 1500 km. The signal at 638ms is from the aurora at 3900 km. Signal at 664ms is a Doppler shifted version of the signal at 638ms. Signal at 752ms is the first around the world at 41,850 km.

To verify what was happening, the radar was put into CW mode to measure the Doppler shift which is shown in Figure 11. The Doppler shift shown in Figure 11 can be used to calculate the range error of +26 ms on 28 MHz (a negative Doppler shift gives a positive range error). This shifts the Doppler signal back to exactly the position of the non-Doppler shifted backscatter signal thus verifying that the Doppler shifted signal results from the same area as the backscatter signal at 3900 km.

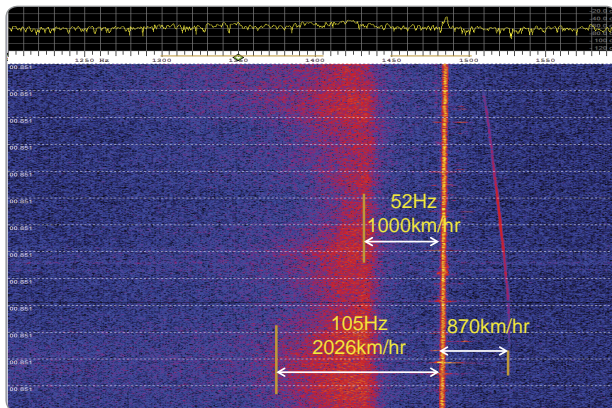


Figure 11: 28 MHz chirp backscatter radar measurements at 220 degrees, 04:40UTC, 29 June 2012. Solar wind at the time was around 600 km/sec resulting in an unsettled geomagnetic field and associated extended auroral oval. The direct signal with no Doppler shift is shown as the bright line at 1485Hz. The curved line to the right of the direct signal is an aircraft travelling at a maximum line of sight speed of 870 km/hr. The bright area to the left of the direct signal is the auroral Doppler shifted backscatter signal that has a line of sight velocity of between 1000 km/hr and 2026 km/hr.

The unsettled geomagnetic field at the time resulted in a strong movement of plasma away from the radar in the ionosphere which gives rise to the negative Doppler shift. Pointing the antennas further South resulted in a reduction of the radar return level from the auroral oval.

Strong, field aligned upward flow velocities of O+ at times approaching horizontal velocities of 1 km/second (3600 km/hr) are frequently observed in the F region. There are indications in Figure 11 that velocities approaching 3000 km/hour could be present. The Super DARN radar was set up to measure the auroral effects seen here and a good source of information can be obtained from [23] as well as the many other readily available.

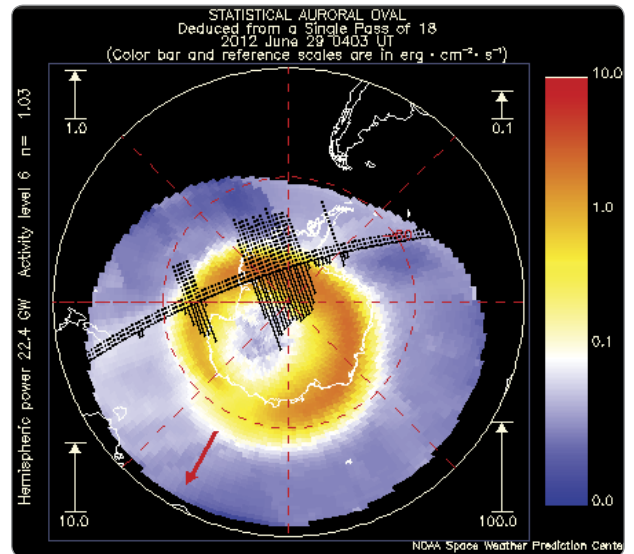


Figure 12: Satellite measurement of the Southern auroral oval at 04:03UTC, 29th June 2012. The positions of the Es return and the Auroral return in the direction of 220 degrees are shown.

To measure to a distance of 3900 km requires that the radar signal is refracted by the ionosphere as the reflection from the ionospheric plasma irregularities is at a height of around 200 km which is not sufficiently high to be visible by line of sight. This is probably the first time that amateur radar technology has been used to measure Doppler effects from the auroral oval. I have offered only a brief description of the effects being measured as the details are much more complex and are the subject of much on-going research.

Conclusions

The chirp and CW radar has been used successfully in a number of modes to look at various propagation modes relating to Es and F layer propagation. For distances up to 11,000 km, nEs is shown to be a viable mode. It is also probable that nEs is responsible for many northern and southern hemisphere 50 MHz contacts. If this is the case, then the concerns about signal distortion and

excessive path loss with nEs propagation [14, 16] are unfounded. If the nEs mode is viable over the distances measured by the radar then it is entirely possible that the long distance VK/NA Winter/Summer solstice 50 MHz contacts are by nEs. It should thus be possible to make nEs contacts between VK and Europe on 50 MHz without the need to wait for the sun to deliver every 11 years.

It is also reasonable to assume that good radar returns on 28 MHz will indicate the possibility of 50 MHz nEs openings.

Around-the-world results on 28 MHz raise the possibility for investigating this mode on 50 MHz.

This work also shows that new discoveries and measurements can still be made by amateurs and that there are 50 MHz propagation opportunities still waiting to be explored. To take up these opportunities good antennas and higher power with common worldwide band plans would greatly assist especially given the propagation losses involved. It is also essential that the section of the 50 MHz band between 50.10 and 50.15 be kept entirely free from QRM caused by local VK/ZL Es contacts. This section of the band should be only for contacts between VK and the rest of the world.

Acknowledgement

I wish to thank Roger Harrison VK2ZRH for critically reviewing this article as well as providing many of the very helpful references.

References

1. A. Martin, "Backscatter Radar", <http://vklogger.com/forum/viewtopic.php?f=29&t=9002>.
2. A. Martin "A Bistatic Backscatter Chirp Radar For Amateur Radio Use", DUBUS, 2/2010, pp 24-39.
3. Spectrum Lab, <http://www.qsl.net/dl4yh/spectra1.html>
4. A. Martin, "Adventures With A Radar, Es Backscatter Doppler Shift Measurements Using CW and Chirp Radar Techniques", GippsTech 2012, to be published in 2013.
5. P. Harman, VK6APH, "The Chirp Beacon Mode, A novel way to get high gain from a beacon transmitter, DUBUS, 4/2011, pp 45-48.
6. <http://openhpsdr.org/publications.php>
7. R. Harrison, "Sporadic E – MUF Myths, Summer Solstice Short Path Propagation and Forecasting Openings", Proceedings of GippsTech 2011, pp 91 to 123.
8. <http://vklogger.com/>
9. R. Harrison VK2ZRH, Sporadic E: turmoil, turbulence and torment, Proceedings from the GippsTech Conference 2007.
10. http://en.wikipedia.org/wiki/Kelvin-Helmholtz_instability

11. R.K. Choudhary and J.-P. St.-Maurice, "Quasi-periodic backscatters from the E region at Gadanki: Evidence for Kelvin-Helmholtz billows in the lower thermosphere?", Journal of Geophysical research, Vol. 110, A08303, doi:1029/2004JA010987, 2005, pp 1-19.
12. P.A Bernhardt, J. Werne, and M.F. Larsen 2006, "Modelling of Sporadic-E Structures from Wind-Driven Kelvin-Helmholtz Turbulence", Characterising the Ionosphere, Meeting Proceedings RTO-MP-IST, Paper 34, pp 34-1 – 34-14. At <http://ftp.rta.nato.int/public/PubFullText/RTO/MP/RTO-MP-IST-056/MP-IST-056-34.pdf>
13. W.R. From and J.D. Whitehead, "Es Structure Using an HF Radar", URSI-IPS Conference on the Ionosphere and Radio Wave Propagation, 1985. courtesy of Roger Harrison, VK2ZRH.
14. J. Kennedy and G. Zimmermann, "Extreme Range 50 MHz Es: East – West (EWEE)", DUBUS, 1/2012, pp 51 – 62.
15. K. Siwiak, "Optimum Height for an Elevated Communications Antenna", DUBUS, 3/2010, pp 86 – 93.
16. H. Higasa, JE1BMJ, "SSSP: Short-path Summer Solstice Propagation", at http://www.ha5hrk.hu/files/SSSP_JE1BMJ.pdf
17. H.A. Hess, "Investigations of High-Frequency Echoes", Proc. IRE, 36, 1948, pp 981 – 992.
18. Carera et al, "Guided Propagation of HF Radio Waves in the Ionosphere", Space Science Reviews, 11, 1970, at: <http://adsabs.harvard.edu/full/1970SSRv...11...555C> See page 557.
19. HamCap <http://www.dxatlas.com/HamCap/>
20. J. A. Harvey, 1955, "Movement of sporadic E ionization", Australian Journal of Physics, Vol. 8(4), pp 523–534; at: www.publish.csiro.au/paper/PH550523.htm
21. R.B. Fenwick and O.G. Villard Jr, "Time Variation of Optimum Azimuth for H-F Around the World Propagation", Radioscience Laboratory, Stanford Electronics Laboratories. At: <http://www.dtic.mil/cgi-bin/GetTRDoc?AD=AD0274274>
22. Steele, J. G., "Backscatter of 16Mc/s Radio Waves by Land and Sea", Aust. J. Phys., 1965, 18, pp 317 – 327.
23. http://www.cawcr.gov.au/publications/technicalreports/CTR_045.pdf

Endnotes

- 1 VK3OE@bigpond.com. Copyright A. Martin 2012.
- 2 I have not found any information on the backscatter correlation coefficients of the Es ripples or for the earth surface for the context in which it is applied here.